Advances in Science and Technology Research Journal

Advances in Science and Technology Research Journal, 2025, 19(1), 72–87
https://doi.org/10.12913/22998624/194607
ISSN 2299-8624, License CC-BY 4.0

Received: 2024.09.29
Accepted: 2024.11.15
Published: 2024.12.01

Flexural strengthening of reinforced concrete beams using carbon fiber reinforced polymer rope with additional anchorage to limit debonding

Paweł Tworzewski[1*], Kamil Bacharz[2]

[1] Department of Building Structures, Kielce University of Technology, Al. Tysiąclecia Państwa Polskiego 7, 25-314 Kielce, Poland

[2] Department of Strength of Materials and Structures Diagnostics, Kielce University of Technology, Al. Tysiąclecia Państwa Polskiego 7, 25-314 Kielce, Poland

* Corresponding author's e-mail: ptworzewski@tu.kielce.pl

ABSTRACT

The use of CFRP rope as NSM flexural strengthening and at the same time a method of limiting its debonding by anchoring its ends in drilled holes was described. The work examined the effectiveness of strengthening reinforced concrete beams using NSM CFRP ropes and compared the solution with the traditional one using NSM CFRP strips. The study included 14 elements, including: 3 unstrengthened beams, 5 beams strengthened with NSM CFRP ropes and 6 beams strengthened with NSM CFRP strips. All beams were loaded monotonically until failure with two concentrated forces (four-point loading testing). The measurements were carried out using digital image correlation (DIC). In order to limit the possibility of debonding, an anchorage made of CFRP rope glued into previously drilled holes in the beam web at an angle of 90° (6 beams) and in the case of using two CFRP ropes, at an angle of 45° and 90° (2 beams) was used in selected beams. The analysis included a comparison of: failure modes, load–deflection responses and strain distributions. The obtained value of strengthening efficiency was: with the use of a single rope 25–30%, with the use of two ropes 46 and 49%, for CFRP strip 31–36%. In the case of the beams strengthened with CFRP rope, debonding did not occur. In all beams strengthened with CFRP strips, debonding occurred and the additional anchoring did not contribute to the delay of its occurrence. All beams reinforced with CFRP rope achieved higher load-bearing capacity than expected and in no case failed due to debonding, which means that the assumed objectives of the work were met.

Keywords: debonding, flexural strengthening, CFRP rope, concrete, near-surface mounted (NSM).

INTRODUCTION

Modern construction is based on many advanced technologies. Material issues concerning both reinforced concrete and concrete structures [1], the use of alternative reinforcement methods, e.g. dispersed reinforcement and strengthening of the structure can be mentioned here. In parallel, diagnostic methods are developing, which are necessary in determining the technical condition of existing structures, e.g. galvanostatic methods [2] to assess corrosion of metallic reinforcement, or acoustic methods to assess the general condition of the structure [3, 4]. The aforementioned diagnostics of building structures is extremely important, especially in terms of maintaining buildings in a suitable condition allowing for their con stant use. This is often associated with the need to interfere with the structure, e.g. with the need to strengthen the structure.

Several failure modes of RC beams strengthened with FRP plates, strips or sheets can be distinguished. The first mechanism is intermediate crack debonding [5]. When it occurs within the interfacial concrete, there are no efficient methods to avoid this failure [6, 7]. Therefore, it is extremely important to control this mechanism, especially in the case of slender elements strengthened with thin FRP plates or sheets, which are particularly exposed to this type of failure. The second mechanism consists of steel yielding followed by rupture of the composite reinforcement in the middle of the element. Other mechanisms include steel yielding, followed by crushing of compressive concrete, loss of anchorage at composite ends, which includes plate end debonding (delamination of the FRP material from the concrete element which starts from the end [8, 9], concrete cover separation (debonding of FRP material together with the concrete cover of the reinforcing steel, mainly starting from one end and moving toward the element center [10–12] and anchorage failure if it is used [13, 14].

In the case of RC members strengthened with an externally bonded CFRP plate or sheet reinforcement (EBR) [15], or spent catalyst based ferrocement laminates [16], one of the problems is debonding from the concrete surface, which leads to premature failure. In this case, the process of correct preparation of the surface of the strengthened element before gluing the FRP material is very important. When correctly carried out, it can contribute to delaying the debonding of the reinforcement and obtaining a higher ultimate final strength. Of course, the basic activities include: removing loose concrete, leveling the concrete surface to avoid unevenness typical in this case, removing any contamination from both the concrete surface and the FRP material. It should be remembered that the epoxy resin should also be clean and free from external materials. Additional procedures described in this paper [17] such as transverse, diagonal, and longitudinal grooving creates the higher contact area may also delay the moment of debonding of the FRP material.

One of the solutions to limit debonding is to increase the surface interacting with the strengthened element by gluing composite reinforcement into the cover. This type of reinforcement is called near surface mounted reinforcement (NSM) or side near surface mounted (SNSM) technique, depending on the location of the reinforcement. The preparation itself requires making a groove in the concrete cover of the element, which in fact limits the long-term surface preparation that is necessary in the case of the EB technique [18]. There is a risk of damaging the existing reinforcement. Therefore, this method can only be used in the cases where the thickness of the concrete cover of the reinforced element allows it. This technique significantly increases the effectiveness of the reinforcement and allows for obtaining higher ultimate strengths. [19, 20]. Since the reinforcement is glued into the groove, it is possible to use not only strips, but also FRP bars or fiber cords. It should be emphasized that the NSM technique does not eliminate the possibility of debonding, but only limits it. In this case, studies show two main mechanisms of debonding of the FRP material from the reinforced concrete element, both initiated at the end of the FRP material [21–23]. In the first mechanism, normal stresses and high shear at the contact of the two materials lead to cracks in the FRP-concrete interface, which ultimately lead to debonding of the FRP material [24–26]. In the second mechanism, the concrete cover is separated together with the FRP material, initiated by a crack near the end of FRP (Fig. 1) [27–30].

Research is still ongoing on methods that allow for delaying or eliminating the failure mechanisms described above, related to

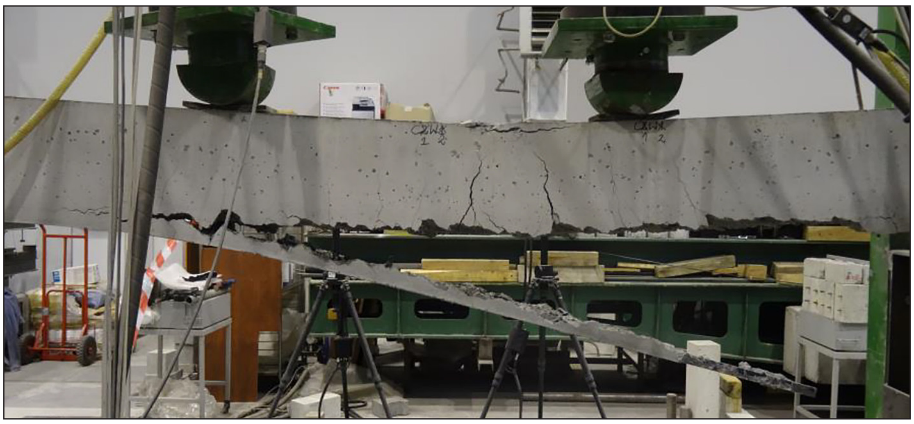

Figure 1. Concrete cover separated together with the FRP material, initiated by a crack near the end of the FRP strip [26]

debonding. These methods consist in improving the anchoring of the FRP material at its end. An example is the use of FRP U-jackets. This is a well-known method, the results of which have been described in many works. This is a solution used simultaneously with shear reinforcement [15, 31–33]. In the case of composite sheets, it is possible to improve the anchoring by gluing its end into a previously made groove and placing a composite rod there (Fig. 2b). This method was presented in [34]. Although it is mainly intended for shear strengthening, its application is also possible in the case of bending strengthening of reinforced concrete beams.

The method for anchoring composite materials is also the use of steel anchoring elements. The effectiveness of this type of solution is widely known. Currently, such solutions are used in the case of prestressed FRP composites for concrete structures [14, 35].

The use of composite anchors combined with substantial reinforcement allows eliminating the largest defect of anchorages based on steel elements, i.e. corrosion susceptibility. The work [36] presents a 30% increase in load capacity for elements with additional composite anchors. Composite anchors are made of fiber cords, glued into previously drilled holes in the beam web. These holes are most often made perpendicular to the anchored reinforcement, e.g. a composite sheet. To obtain a connection between two materials, part of fiber cords left outside is fan-folded on the surface (Fig. 2a).

An interesting modification of this method is presented in [21]. It consists in using a sleeve made of fiber sheet, wrapped at the end with NSM strip and steel wire (Fig. 3). This wire facilitates insertion of fiber sheet into a previously drilled hole at a given angle. The presented research results show that the use of EFAs led to an increase in the load-carrying capacity of the NSM-strengthened beam by 13% to 35%. For comparison, the use of FRP U-jackets showed an increase of only 9%.

The use of NSM – CFRP rope for reinforcing steel beams as presented in [37], unlike the rigid NSM strip, allows for any shaping of the composite material course. In this case, the rope was glued into previously made grooves on both side walls of the beam with a variable course. In the support zone, the grooves were not horizontal, but inclined at a specific angle of 15, 20 or 45 degrees. Additionally, the end of the rope was anchored by gluing into a drilled hole. The use of this solution eliminates the need to connect different materials in order to perform the anchoring.

In summary, limiting the debonding phenomenon, which leads to premature failure, is still a great challenge. Simple, durable, effective and cheap to implement methods are sought.

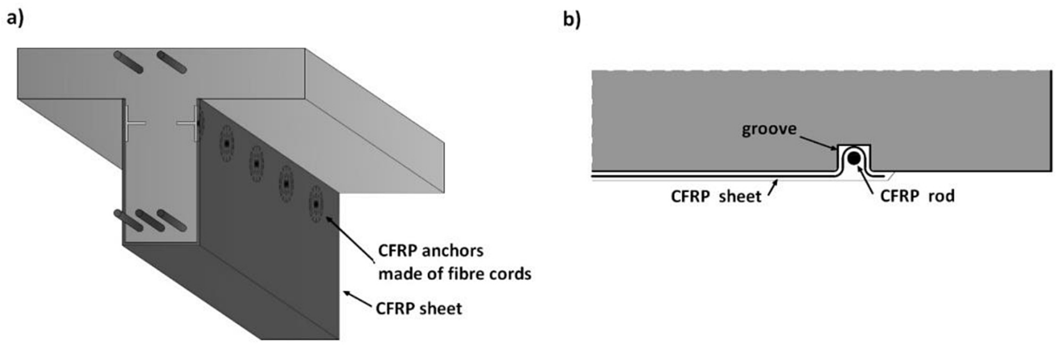

Figure 2. Anchoring of the FRP reinforcement end: (a) using a composite anchor, (b) using a groove and a transversely positioned FRP rod

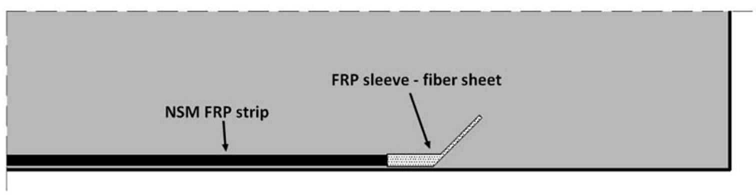

Figure 3. The use of sleeve made of fiber sheet, wrapped at the end with NSM strip to delay debonding

CONCEPT AND ASSUMPTIONS

The authors used a CFRP rope as a bending reinforcement and at the same time anchored its ends in order to limit the possibility of failure through debonding. This concept is presented in Figure 4. This method uses and combines the most important features of the solutions presented above, namely: strengthening using the NSM method, the possibility of trouble-free anchoring and prevention of premature debonding, the possibility of simultaneously performing strengthening for bending and shear, no steel elements, no connections. This method, compared to the use of FRP U-jackets, does not require such complicated preparation of the concrete surface. In addition, the anchorage glued inside the beam web is not itself exposed to debonding like the sheet used for FRP U-jackets. The method proposed in [21] requires combining materials and complicated preparation of the anchorage before its application to the element. In most cases, the method of anchoring the CFRP rope presented in [37] cannot be used in real elements due to limited access to the element at the support. The use of the proposed method for strengthening the beam in shear was not tested in this work, but it is possible. The idea is similar to the one presented in [38], where composite bars were glued at different angles into the web of a reinforced concrete beam. Proposed solution was compared with the traditional one, i.e. strengthening using NSM CFRP strip.

The study planning began with the selection of parameters of the materials from which the beams were made and the CFRP materials used for strengthening (Fig. 5). They were assumed so that the predicted failure model for each of the strengthened beams was debonding. This involved, among other things, the adoption of a concrete class so as to limit the possibility of failure by concrete crushing in the compression zone. Calculations for this purpose were performed based on the ACI standard, specifying the failure model: due to concrete crushing, FRP rupture or debonding (for debonding effective strain in FRP reinforcement limited to $0.7f_f/E_f$). The CFRP strip was selected to obtain the same composite reinforcement ratio $\rho_{f,eq}$ as in the case of beams reinforced with CFRP rope. Additionally, for two beams, strengthening was performed with two CFRP ropes, owing to which the predicted load-bearing capacity value was obtained similar to the beams strengthened with CFRP strip. For two beams strengthened with CFRP strips, additional anchoring was performed using a CFRP cord. This sample preparation was intended to facilitate the effectiveness evaluation of the proposed strengthening concept in relation to alternative methods and to check whether premature debonding could be prevented.

SPECIMENS AND THEIR PREPARATION

The results concern the tests of 14 single-span reinforced concrete beams with a total length of 3.3 m (distance between the axes of supports 3.0 m) and a rectangular cross-section of 0.3 × 0.12 m. The beams were equipped with two Ø14 reinforcing bars as lower reinforcement and two Ø8 as upper reinforcement, all made of B500SP steel. The reinforcement ratio of steel bars was $\rho_s = 0.93\%$ (Fig. 6). During concreting, cube-shaped samples were taken: 150 × 150 × 150 mm. Two concrete mixtures of different strength classes were used to prepare the beams. The beams marked with the

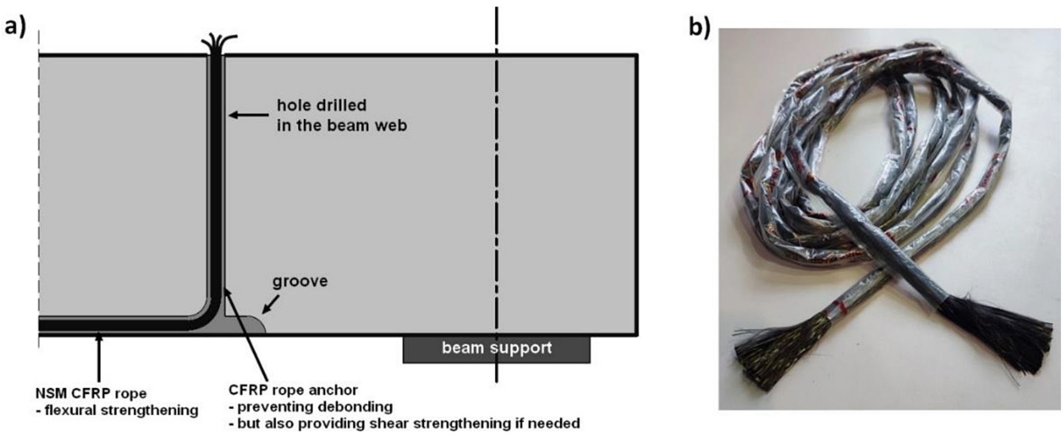

Figure 4. (a) Schematic concept representation of strengthening and anchoring of the CFRP rope, (b) CFRP rope

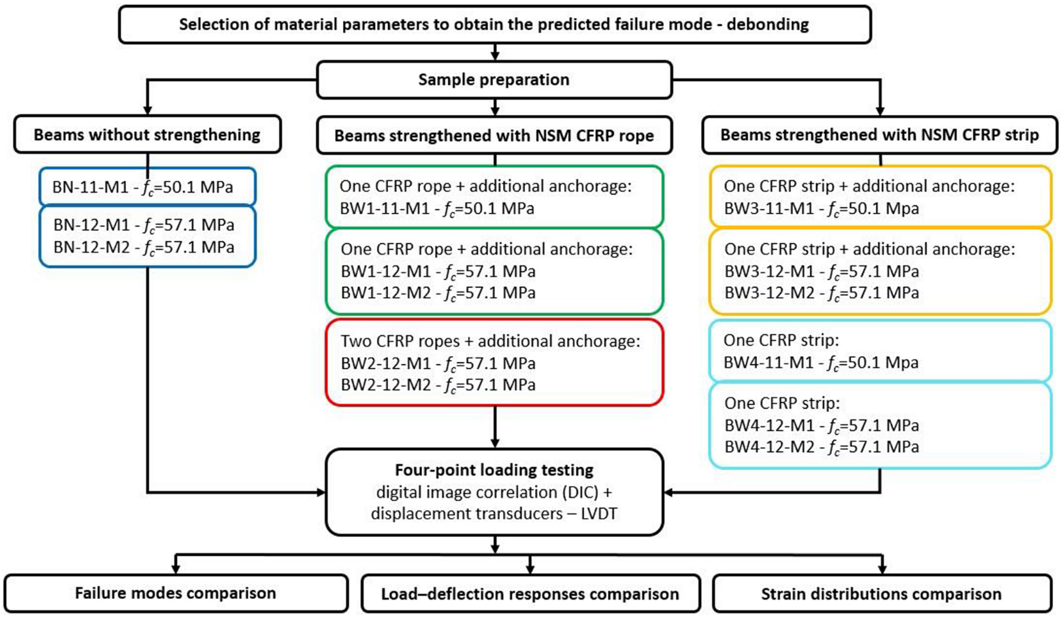

Figure 5. Flowchart of the research methodology

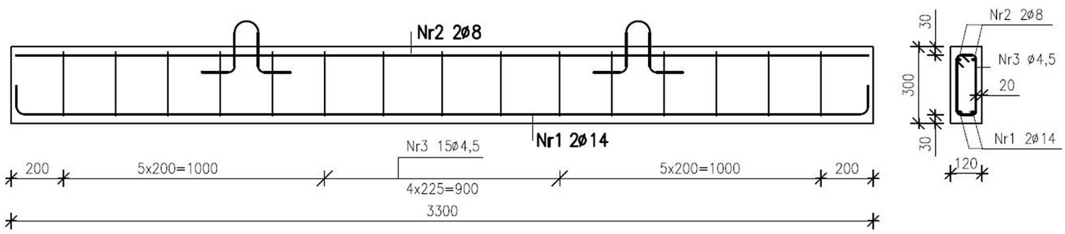

Figure 6. Reinforcement scheme of test beams

symbol 11 were made of concrete with an average strength of f_c = 50.1 MPa (cylinder compressive strength) determined on the basis of tests of 12 samples. In the case of the beams with the symbol 12, an average strength of f_c = 57.1 MPa was obtained on the basis of tests of 36 samples. The strength of the applied main reinforcement was determined on the basis of a tensile test carried out for 42 samples.

Three beams marked with the symbol BN are reference elements, without strengthening. The remaining beams were strengthened in four different ways:

- I type (BW1) – 3 beams reinforced with CFRP SikaWrap FX-50C rope embedded in epoxy resin in pre-cut grooves in the concrete cover (Near Surface Mounted Reinforcement). In order to ensure proper anchoring, the ends of the rope were placed in vertical holes made in the support zones (Fig. 7). The carbon fibers were impregnated along their entire length with Sikadur -52 resin. Sikadur -330 resin was used to fill the previously cut grooves (width 1 cm, depth 2 cm) and vertically drilled holes (diameter 2 cm). The obtained composite reinforcement factor was ρ_f = 0.08%.
- II type (BW2) – 2 beams reinforced with 2 CFRP SikaWrap FX-50C ropes embedded in epoxy resin in pre-cut grooves in the concrete cover (Near Surface Mounted Reinforcement). In order to ensure proper anchoring, the ends of the rope were placed in holes made in the support zones: vertical holes for the first rope and made at a 45-degree angle for the second rope (Fig. 7). The carbon fibers were impregnated along their entire length with Sikadur -52 resin. Sikadur -330 resin was used to fill the previously cut grooves (width 1–1.5 cm depending on location, depth 2 cm) and drilled holes (diameter 2 cm). The obtained composite reinforcement factor was ρ_f = 0.16%.
- III type (BW3) – 3 beams reinforced with Sika CarboDur S NSM 1.525 CFRP strip embedded in epoxy resin in pre-cut grooves in the concrete

cover (Near Surface Mounted Reinforcement) with additional anchorage made of SikaWrap FX-50C CFRP rope (Fig. 7). The carbon fibers of the rope were impregnated along the entire length with Sikadur -52 resin. Sikadur -330 resin was used to fill previously cut grooves (width 1 cm, depth 2 cm) and drilled holes (diameter 2 cm). The obtained composite reinforcement factor was ρ_f= 0.11%.
- IV type (BW4) – 3 beams reinforced with Sika CarboDur S NSM 1.525 CFRP strip embedded in epoxy resin in pre-cut grooves in the concrete cover (Near Surface Mounted Reinforcement) without additional anchoring (Fig. 7). Sikadur -330 resin was used to fill the previously cut grooves (width 1 cm, depth 2 cm). The obtained composite reinforcement ratio was ρ_f = 0.11%.

Detailed data on the specimens and their strengthening are presented in Table 1 and Figure 7. The beams were tested after a minimum of 30 days from the moment of their strengthening, so that the resin could obtain its target strength. The testing of cubic samples was carried out so that they overlapped in time with the testing of the corresponding beams. The exact dates of concreting, strengthening and testing of the beams are given in Table 2.

Before gluing the reinforcement, the beams were grooved in a horizontal position using a groover machine (Fig. 8). The groove dimensions were adopted in accordance with the manufacturer's requirements (Fig. 9). Then, similarly to the drilled holes, loose pieces of concrete were removed and cleaned using compressed air to obtain the best possible adhesion. The CFRP strip was glued into a groove previously filled with resin, while in the case of the rope, gluing began by pulling it through a hole drilled in the beam's web filled with resin. For this purpose, a plastic clamp was placed at the end of the rope. Then, a wire was hooked to it and pushed through the hole. While pulling the rope through the hole, the glue was continuously replenished to minimize the risk of leaving empty spaces. The application of the strengthening may seem more difficult because, unlike tapes, it is flexible and difficult to push into a groove filled with resin. However, since the holes in the beam web were

Table 1. Specimen parameters and anchorage details

Specimen	Concrete		Steel bars			Beam strengthening parameters					
	f_c [MPa]	E_c [GPa]	A_{s1} [cm^2]	f_y [MPa]	E_s [GPa]	Typ	A_f [mm^2]	f_f [MPa]	E_f [GPa]	Anchorage angle [°]	$\rho_{f,eq}$ [%]
BN-11-M1	50.1	35.7	3.08	505.8	219.8	-	-	-	-	-	-
BN-12-M1	57.1	37.1	3.08	505.8	219.8	-	-	-	-	-	-
BN-12-M2	57.1	37.1	3.08	505.8	219.8	-	-	-	-	-	-
BW1-11-M1	50.1	35.7	3.08	505.8	219.8	I	28	2000	230000	90	0.08
BW1-12-M1	57.1	37.1	3.08	505.8	219.8	I	28	2000	230000	90	0.08
BW1-12-M2	57.1	37.1	3.08	505.8	219.8	I	28	2000	230000	90	0.08
BW2-12-M1	57.1	37.1	3.08	505.8	219.8	II	28+28 =56	2000	230000	90+45	0.17
BW2-12-M2	57.1	37.1	3.08	505.8	219.8	II	28+28 =56	2000	230000	90+45	0.17
BW3-11-M1	50.1	35.7	3.08	505.8	219.8	III	37.5	3100	170000	90	0.08
BW3-12-M1	57.1	37.1	3.08	505.8	219.8	III	37.5	3100	170000	90	0.08
BW3-12-M2	57.1	37.1	3.08	505.8	219.8	III	37.5	3100	170000	90	0.08
BW4-11-M1	50.1	35.7	3.08	505.8	219.8	IV	37.5	3100	170000	-	0.08
BW4-12-M1	57.1	37.1	3.08	505.8	219.8	IV	37.5	3100	170000	-	0.08
BW4-12-M2	57.1	37.1	3.08	505.8	219.8	IV	37.5	3100	170000	-	0.08

Note: f_c – compressive strength of concrete (cylinder compressive strength); E_c – modulus of elasticity of concrete; A_{s1} – cross sectional area of reinforcement in the tension zone: 2Ø14; f_y – yield strength of reinforcement; E_s – modulus of elasticity of steel; Type I, II, III, IV – determines the method of reinforcing the reinforced concrete beam described above; A_f – cross sectional area of FRP: CFRP SikaWrap FX-50C rope 28 mm^2 (based on carbon fiber content), Sika CarboDur S NSM 1.525 CFRP strip 37.5 mm^2; f_f – tensile strength of the FRP; E_f – modulus of elasticity of FRP; 45°, 90° – drilling angle for anchoring at the end of the FRP reinforcement made of CFRP SikaWrap FX-50C rope; $\rho_{f,eq} = \rho_f E_f / E_s$.

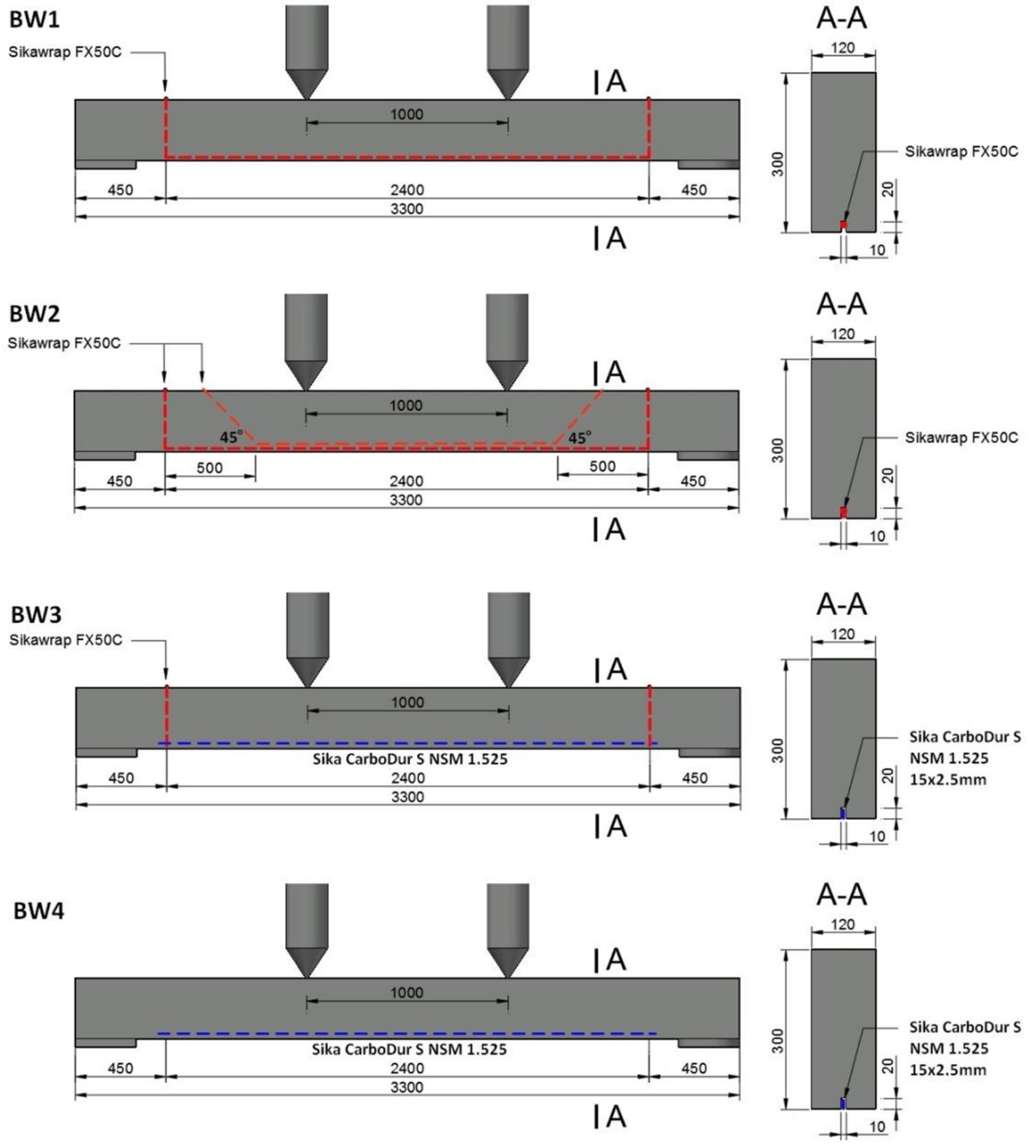

Figure 7. Schemes of strengthening reinforced concrete beams

Table 2. Research schedule

Specimen	Date of beam concreting	Beam strengthening date	Test date
BN-11-M1	12.07.2017	-	21.05.2018
BW1-11-M1		19.02.2018	27.03.2018
BW3-11-M1			27.03.2018
BW4-11-M1			21.03.2018
BN-12-M1	14.07.2017	-	30.11.2017
BN-12-M2			13.02.2018
BW1-12-M1		12.01.2018	13.02.2018
BW1-12-M2			20.02.2018
BW2-12-M1	18.07.2017	29.01.2018	28.02.2018
BW2-12-M2			28.02.2018
BW3-12-M1			01.03.2018
BW3-12-M2			02.03.2018
BW4-12-M1	20.07.2017	9.02.2018	12.03.2018
BW4-12-M2			12.03.2018

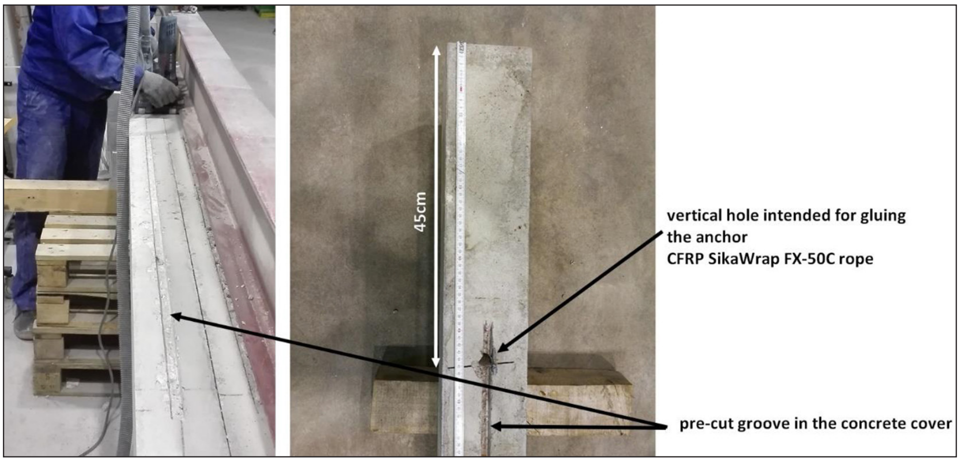

Figure 8. Preparing the beam for gluing reinforcement

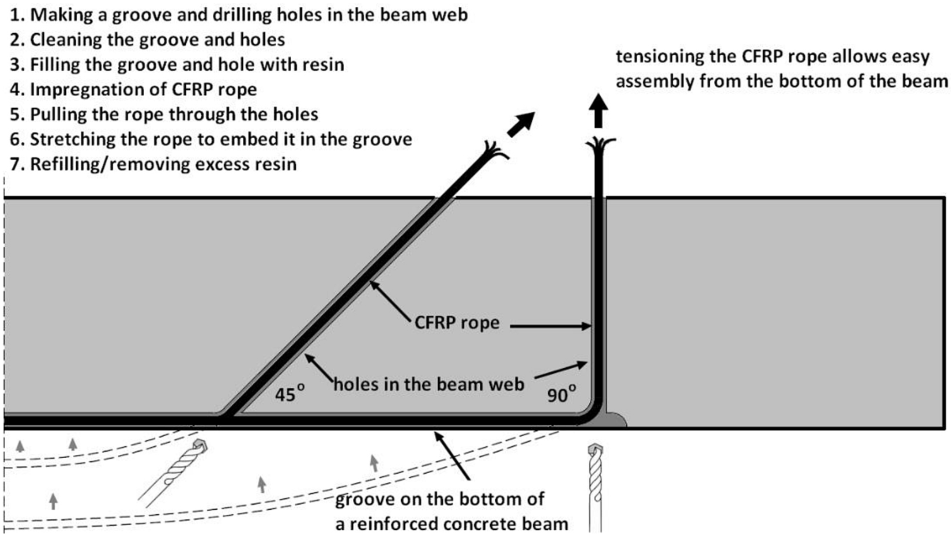

Figure 9. The procedure used to prepare beam strengthening using CFRP rope

drilled through its entire height, it was possible to easily install the CFRP rope and tension it to obtain the correct course in the groove made along the beam. The procedure for gluing CFRP rope is shown in Figure 9.

TEST SETUP

The samples were tested at the setup shown in the Figure 10a, where the support spacing was 3 m and the distance between the actuators was 1 m (four-point loading testing). The measurements were carried out using digital image correlation (DIC) – two ARAMIS 5M system sensors (Fig. 10a) and five displacement transducers – LVDT.

The measurements of strains on the side surface, displacements and observation of crack development were carried out by the DIC system. This is a very versatile system commonly used in laboratory tests [39–41]. To make the measurement possible, the surface of the beam recorded by the cameras was covered with a pattern. Then, auxiliary lines were drawn on the beam in black dashed line: horizontal at the height of the center of gravity of the tension and compression reinforcement, vertical at the middle of the beam span and under the points of force application. Non-coded markers were also glued along the length of the drawn horizontal lines at distances of 20 cm (13 markers on the upper and lower lines). The ARAMIS 5M system used in the study is equipped with a monochrome Baumer TXG50 cameras with a resolution of 2448×2050 pixels and Schneider Kreuznach Cinegon 1.4/12-0906 lenses (Fig. 10b) and the possibility of using two sensors (2 × 2 = 4 cameras) at the same time. In this studies the system recorded one stage every 20 seconds.

Beams were loaded monotonically until failure with two concentrated forces – speed 0.4 kN/min. Additionally, the moment of failure of each beam was recorded by a camera placed on a tripod on the other side of the beam relative to the one recorded by the ARAMIS 5M system.

TEST RESULTS

Failure modes

BW1

All samples of this type failed in a similar manner, i.e. rupture of the CFRP rope followed by concrete compressive crushing on the top surface of the beam (Fig. 11). In the case of beams BW1-11-M1 and BW1-12-M1, the composite rupture and concrete crushing occurred on the side of the P1 actuator, i.e. closer to the sliding support, while in the case of beam BW1-12-M2, the failure occurred on the opposite side. The experimental ultimate loads were also similar for all elements and in each case higher than predicted from the calculations (Table 3). The predicted separation of the CFRP rope did not occur, which may indicate the effectiveness of the applied anchorage. Before the CFRP rope rapture, a significant increase in the crack width was recorded, which was visible on the strain map from the ARAMIS 5M system. For example, on the BW1-12-M1 strain map, for the stage just before the beam was destroyed, a large-width crack with an almost horizontal branch at the height of the concrete cover of the main reinforcement was visible on the left side, under the P1 actuator, i.e. near the place where the CFRP rope rapture took place – Figure 12. The numerical analysis of those beams were presented in [42]

BW2

Both samples failed in a similar manner, i.e. concrete compressive crushing on the top surface of the beam (concrete cover separation for top

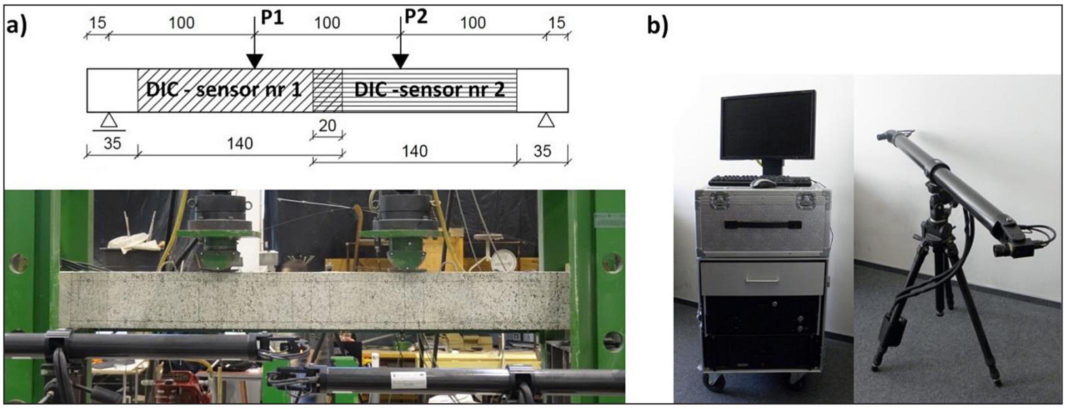

Figure 10. (a) Static scheme of the beam and test stand, (b) ARAMIS 5M system with one sensor

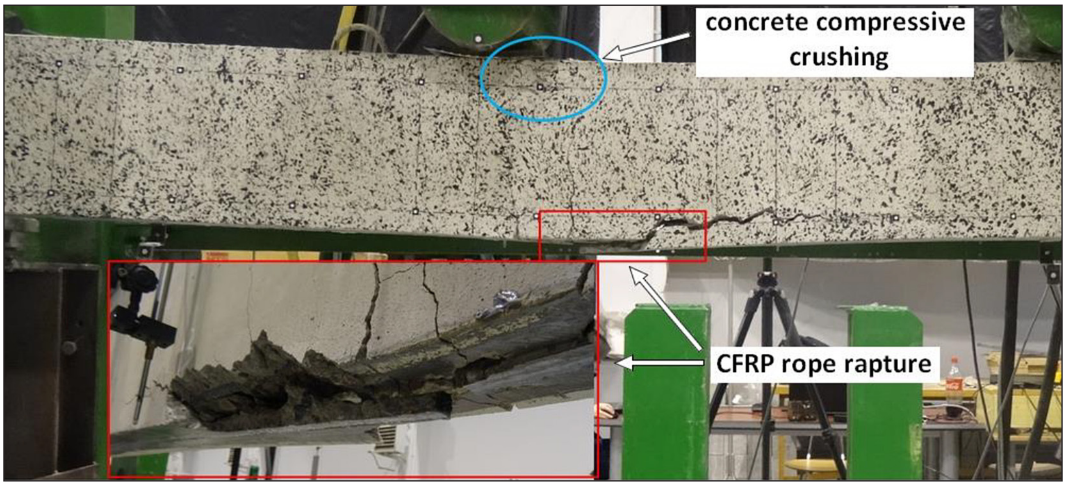

Figure 11. Failure mode of specimen BW1-11-M1

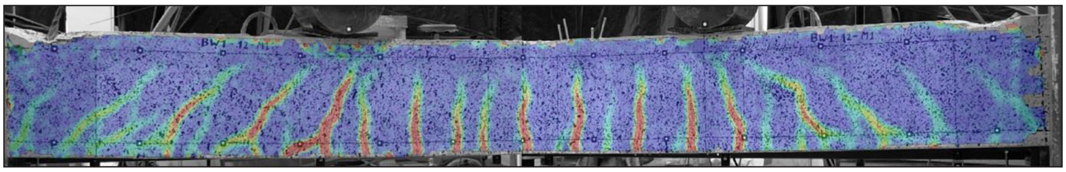

Figure 12. Strain map just before the failure of specimen BW1-12-M1

reinforcement) followed by rupture of the both CFRP ropes (Fig. 13). In the case of beams BW2-11-M1, failure occurred on the side of the P1 actuator, i.e. closer to the sliding support, while in the case of beam BW2-12-M2, the failure occurred on the opposite side. Despite the lower load capacity expected in the calculations than the BW3 and BW4 beams, the experimental ultimate loads and strengthening efficiency η_f were the highest among the tested elements (Table 3). The predicted separation of the CFRP rope did not occur, so this may also indicate the effectiveness of the anchorage. Similar to the BW1 type beams before the failure, an increase in the crack width was recorded, which was visible on the strain map from the ARAMIS 5M system. For example, on the BW2-12-M1 strain map, for the stage just before the beam was destroyed, cracks of greater width (red color) were visible on the left side, under the P1 actuator, i.e. in the place where the failure took place – Fig. 14.

BW3

All specimens failed in a similar manner, i.e. debonding of the CFRP strip initiated at the end of the FRP material (next to the sliding support) followed by concrete compressive crushing on the top surface of the beam (Fig. 15 a). The anchoring of the end made with CFRP rope did not prevent the expected debonding. This may be the result of insufficient contact area between the CFRP strip and CRFP rope. Small decrease in load-bearing capacity can be observed compared to the BW4 type beams. The experimental load-bearing capacity of the beams was lower than that predicted from the calculations (Table 3).

BW4

All specimens failed in a similar manner, i.e. debonding of the CFRP strip initiated at the end of the FRP material (next to the sliding support) followed by concrete compressive crushing on

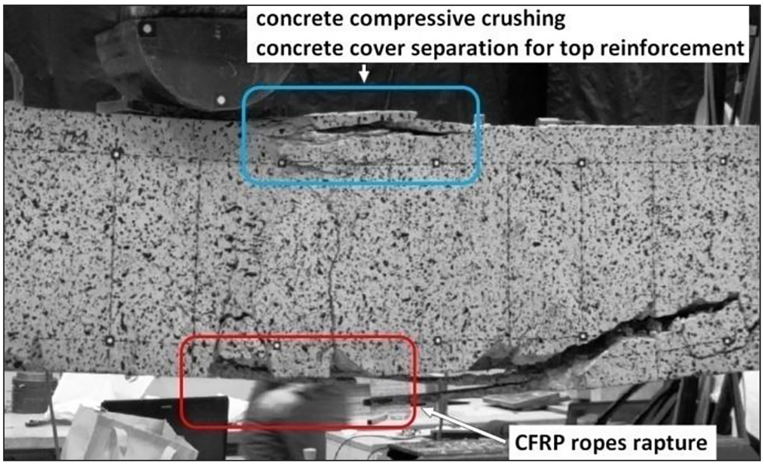

Figure 13. Failure mode of specimen BW2-12-M1

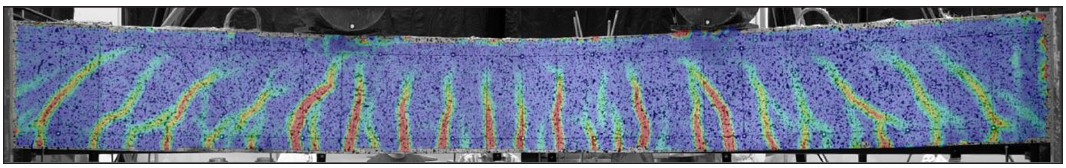

Figure 14. Strain map just before the failure of specimen BW2-12-M1

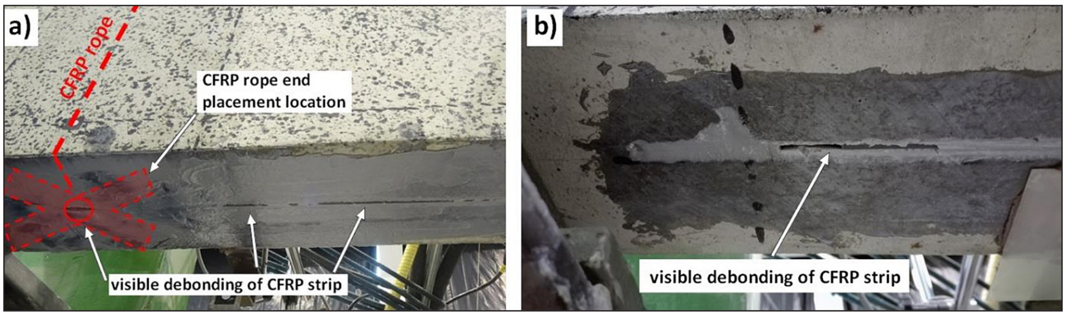

Figure 15. Failure mode of specimen: (a) BW3-12-M1; (b) BW4-12-M1

the top surface of the beam (Fig. 15 b). Failure to do so was consistent with the predicted model and was due to the lack of anchoring of the CFRP end. The experimental load-bearing capacity of the beams was lower than that predicted from the calculations (Table 3). On the basis of the recorded force values, the strengthening efficiency η_f was calculated using formula (1). The results are presented in Table 2.

$$\eta_f = \frac{F_u - F_0}{F_0} \times 100\% \tag{1}$$

where: F_u – ultimate force for the strengthened beam, F_0 – ultimate force for the reference beam – unstrengthened.

Load–deflection responses

The load versus midspan deflection responses for all elements are shown in Figure 16, while the values of maximum deflection and ultimate load are given in Figure 17 and Table 3. It can be observed that for all beams with the same composite reinforcement ratio $\rho_{f,eq}$ = 0.08%, i.e. beams of type BW1, BW3 and BW4, the course of the relationship between force and midspan deflection was practically the same. Differences will appear in the maximum values achieved, i.e. beams BW3 and BW4, due to the significantly higher strength of the CFRP material used, achieve higher load-bearing capacity and, consequently, higher maximum

Table 3. Failure modes and beam load-bearing capacities

Specimen	Predicted (ACI 440.R2-17 [43])		Experimental			
	Ultimate load [kN]	Failure mode	Ultimate load [kN]	Failure mode	η_f [%]	Maximum deflection [mm]
BN-11-M1	-	-	42.8	-	-	56.4
BN-12-M1			44.0	-	-	46.4
BN-12-M2			43.8	-	-	40.8
BW1-11-M1	48.0	Debonding of the CFRP followed by concrete compressive crushing on the top surface of the beam	55.5	Rupture of the CFRP rope (under P1 force) followed by concrete compressive crushing on the top surface of the beam	30	31.1
BW1-12-M1	48.3		55.5		26	32.5
BW1-12-M2			54.9	Rupture of the CFRP rope (under P2 force) followed by concrete compressive crushing on the top surface of the beam	25	29.2
BW2-12-M1	58.2		63.9	Crushing of compressive concrete (under P1 force)	46	38.4
BW2-12-M2			65.3	Crushing of compressive concrete (under P2 force)	49	32.6
BW3-11-M1	59.2		56.9	Debonding of the CFRP strip initiated at the end of the FRP material (next to the sliding support) followed by concrete compressive crushing on the top surface of the beam	33	41.3
BW3-12-M1	59.7		57.9		32	37.6
BW3-12-M2			57.5		31	36.1
BW4-11-M1	59.2		58.4	Debonding of the CFRP strip initiated at the end of the FRP material (next to the sliding support) followed by concrete compressive crushing on the top surface of the beam	36	38.3
BW4-12-M1	59.7		58.6		33	58.3
BW4-12-M2			59.1		35	37.7

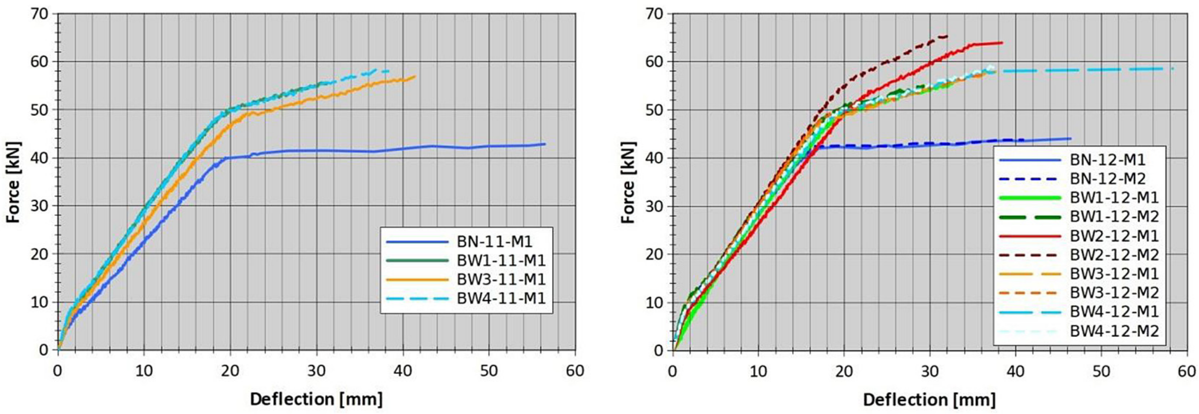

Figure 16. The load versus midspan deflection responses for tested reinforced concrete beams

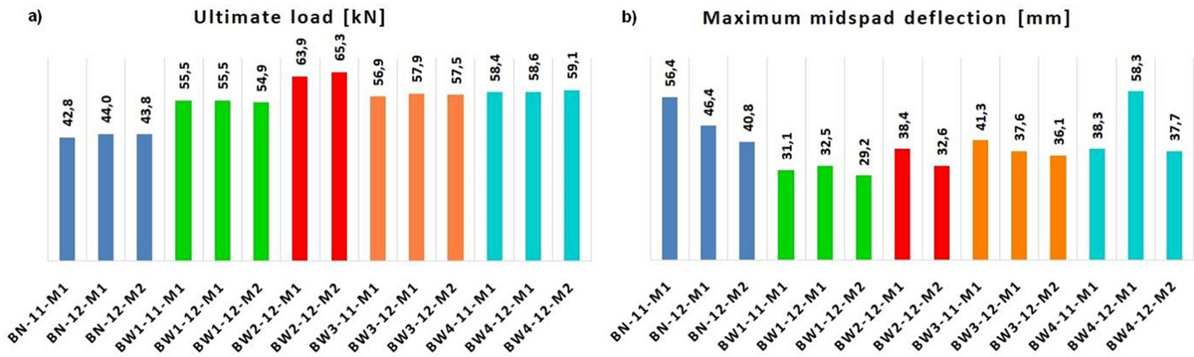

Figure 17. (a) Ultimate load, (b) maximum midspan deflection values for tested reinforced concrete beams

deflection. Beams of type BW2 are characterized by a smaller increase in deflection after the first breakdown of the relationship between force and midspan deflection, i.e. at the moment of reaching the yield point of the tensile reinforcing bars. This results from the highest composite reinforcement ratio of all beams, which amounts to $\rho_{f,eq} = 0.17\%$. At the same time, the course of the described relationship differs significantly between the two beams of this type. The additional anchoring in the BW3 beams did not bring the desired result. On the contrary, the results for the BW4 beams indicate approximately 2% higher load-bearing capacity and approximately 16% greater maximum deflection than in the BW3 beams.

Strain distributions

Continuing the analysis of the discussed beams, an attention should also be paid to the strain distribution recorded up to the center of gravity of the tensile reinforcement (Fig. 18 and 19). For type 12 beams (different compressive strength of concrete compared to type 11 beams), the deformation values were averaged.

In the case of BW1-11-M1 and BW1-12-ŚR beams, it can be observed that the strain values are comparable (BW1-11-M1) or significantly lower (BW1-12-ŚR) than the values for unstrengthened beams. This, as well as the increase in load-bearing capacity (25–30%), results from the increase in the stiffness of the element.

This relationship is different in the case of BW2-12-ŚR beams. In this case a greater increase in load-bearing capacity of approx. 48% was obtained than for BW1 type beams. At load levels in the range of 30–70% relative to failure load, the strain values were higher than for unstrengthened and BW1 type beams, but did not exceed 5‰ before failure. The obtained values were lower than in the case of beams BW3 and BW4. This may be due to the significant stiffening of the support zone, in which not one but two CFRP ropes were anchored, where one of them was trajectory led, due to which greater strains appeared in the central part.

For the same load value in the BW1 and BW2 type beams, for example 49 kN (which is 90% of the ultimate load for BW1), comparable maximum strain values of about 3‰ can be observed. Hence, the increase of the final strain values is

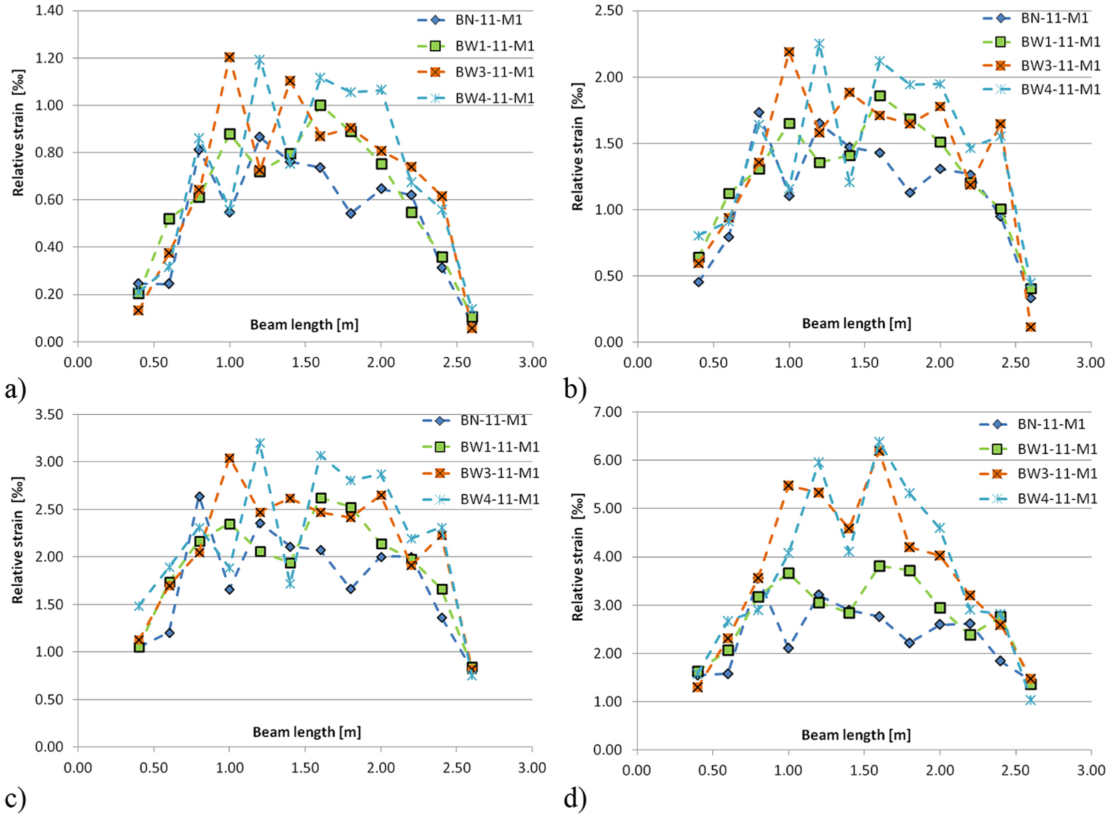

Figure 18. Strain distribution along tensile reinforcement under different percentage of the ultimate load for the type 11 beams, with lower concrete strength (a) 30%, (b) 50%, (c) 70%, (d) 90%

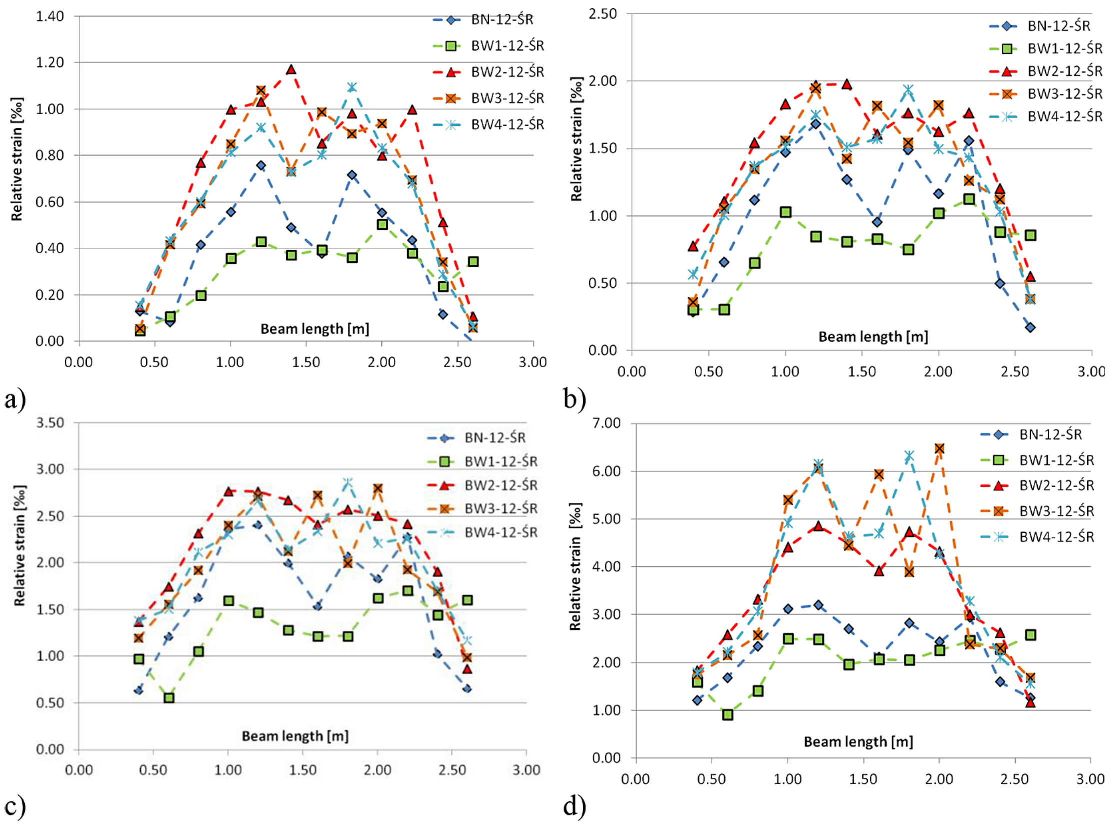

Figure 19. Strain distribution along tensile reinforcement under different percentage of the ultimate load for beams type 12, with higher concrete strength (a) 30%, (b) 50%, (c) 70%, (d) 90%

a result of the higher load-bearing capacity of BW2 beams. In turn, the BW3 and BW4 beams were characterized by similar strain values of the tension zone around 6‰ at the level of 90% of the ultimate load, which, as already described, resulted in the debonding of the CFRP strip initiated at the end of the FRP material regardless of whether it had an additional anchor or not, which was also associated with a decrease in the strengthening efficiency compared to the BW2 beams by about 15%.

In all elements, at 90% of the ultimate load level, increased strain values can be observed in the areas where beam failure occurred.

CONCLUSIONS

The main assumptions of the work, i.e. the use of CFRP rope as an effective method of NSM flexural strengthening of reinforced concrete beams and anchoring its ends in drilled holes in order to limit the possibility of failure through debonding were met. None of the beams reinforced with CFRP rope prematurely failed as a result of debonding. The obtained values of strengthening efficiency are fully satisfactory and compare well with typical methods using CFRP strips. On the basis of the experimental and analytical results, the following conclusions can be drawn:

The obtained value of strengthening efficiency was: for the BW1 type beams strengthened with a single NSM CFRP rope anchored at the ends 25–30%, for the BW2 type beams strengthened with two NSM CFRP ropes anchored at the ends 46 and 49%, for the BW3 type beams strengthened with a NSM CFRP strip with additional anchorage at the end made of a composite anchor 31-33%, while for the BW4 type beams strengthened only with a NSM CFRP strip 33–36%.

The BW1 type beams were destroyed by rupture of the CFRP rope, followed by concrete compressive crushing on the top surface of the beam. The force released during the rupture of the rope caused separation of the concrete bottom covers. The BW2 type beams strengthened with two CFRP ropes failed in a different way. Top concrete cover separation associated with crushing of compressive concrete followed by CFRP ropes rapture could be observed. All beams strengthened with CFRP strip, i.e. BW3 and BW4, failed by strip debonding regardless of the anchoring used – composite anchor at the ends of the strip. The use of a CFRP rope and its anchoring at the ends allowed avoiding failure by debonding, which could not be achieved in the case of beams strengthened with CFRP strip.

For beams BW1, BW3 and BW4 characterized by the same composite reinforcement ratio $\rho_{f,eq}$ = 0.08%, the relationship between force and midspan deflection was practically the same. The differences concern the maximum values of load-bearing capacity achieved and, consequently, the maximum deflection. Beams BW2 characterized by a significantly higher composite reinforcement ratio $\rho_{f,eq}$ = 0.17%, due to their greater stiffness, experienced a slower increase in deflection during the load increase. The average value of the maximum midspan deflection for beams type BW1, BW2, BW3 and BW4 was: 30.9 mm, 35.5 mm, 38.4 mm, 44.7 mm, respectively.

For beams BW1 and BW2 the experimental load-bearing capacity was higher than that calculated based on ACI 440.R2-17 by an average of 13.24%, while for beams BW3 and BW4 it was lower by an average of 2.5%.

To sum up, the results presented above confirm the possibility of effective use of CFRP rope as strengthening of reinforced concrete beams using the NSM method. The studies show that this solution allows for trouble-free execution of effective anchoring and avoidance of failure due to premature debonding.

Of course, the presented studies have their limitations. In order to fully verify the effectiveness of the proposed method, tests should be carried out for the beams strengthened with NSM CFRP rope without anchoring and with consideration of other concrete classes. In order to better reflect the real conditions of CFRP material application, the beams should be subjected to a preload before strengthening so that cracks appear. In order to verify the effectiveness of the solution in terms of strengthening in shear, tests should be carried out for a different static scheme, so as to prevent shear failure in the support zone.

Acknowledgements

The authors would also like to thank Sika Poland sp.z o.o. for the research materials provided. The tests were implemented thanks to the financial support of the Kielce University of Technology within the framework of the statutory work No. 02.0.18.00/1.02.001/SUBB.BKWK.24.003.

REFERENCES

1. Linek M., Nita P., Wolka P., Żebrowski W., Application of Natural Mineral Additives in Construction, IOP Conference Series: Earth and Environmental Science, 2017, 95, https://doi.org/10.1088/1755-1315/95/2/022006
2. Raczkiewicz W., Bacharz M., Bacharz K, Michał T., Reinforcement corrosion testing in concrete and fiber reinforced concrete specimens exposed to aggressive external factors. Materials, 2023, 16, 3, 1-19, https://doi.org/10.3390/ma16031174
3. Bacharz M., Bacharz K., Trąmpczyński W., The Correlation between Shrinkage and Acoustic Emission Signals in Early Age Concrete. Materials. 2022, 15, 15, 5389, https://doi.org/10.3390/ma15155389
4. Goszczyńska B., Świt G., Trąmpczyński W., Tworzewska J., Tworzewski P., Zastosowanie metody emisji akustycznej do analizy procesu zarysowania belek żelbetowych. Zeszyty Naukowe Politechniki Rzeszowskiej, Seria: Budownictwo i Inżynieria Środowiska. 2012, 59, 3/II, 77–84.
5. Tworzewski P., Alexy J.K., Barnes R.W. Intermediate crack debonding of externally bonded FRP reinforcement – comparison of methods. Materials 2022, 15, 7390. https://doi.org/10.3390/ma15207390
6. Ye L.P., Lu X.Z., Chen J.F. Design proposals for the debonding strengths of FRP strengthened RC beams in the chinese design code. In Proceedings of the International Symposium on Bond Behaviour of FRP in Structures, Hong Kong, China, 7–9 December 2005, 45–54.
7. Said H., Wu Z. Evaluating and proposing models of predicting IC debonding failure. Journal of Composites for Construction. 2008, 12, 3, 284–299. https://doi.org/10.1061/(ASCE)1090-0268(2008)12:3(284)
8. Taljsten B. Concrete beams strengthened for bending using CFRP-sheets. In Proceedings of 8th International Conference on Advanced Composites for Concrete Repair, Engineering Technics Press, London, England, 1999.
9. Liu I., Oehlers D.J., Seracino R. Parametric study of intermediate crack IC debonding on adhesively plated beams. In Proceedings of FRP Composites in Civil Engineering, London, England, 2004, 515–521.
10. Sharif A., Al-Solaimani G.J., Basunbul I.A., Balauch, M.H., Ghaleb B.N. Strengthening of initially loaded reinforced concrete beams using FRP plates. ACI Structural Journal. 1994, 91, 2, 160–168. https://doi.org/10.14359/4594
11. Ritchie P.A., Thomas D.A., Lu L.W., Connely G.M. External reinforcement of concrete beams using fiber reinforced plastics. ACI Structural Journal. 1999, 88, 4, 490–500.
12. Nguyen D.M., Chan T.K., Cheong H.K. Brittle failure and bond development length of CFRP—Concrete beams. Journal of Composites for Construction, 2001, 5, 1, 12–17. https://doi.org/10.1061/(ASCE)1090-0268(2001)5:1(12)
13. International Federation for Structural Concrete (FIB). Externally Bonded FRP Reinforcement for RC Structures. Bulletin 14; International Federation for Structural Concrete (FIB): Lausanne, Switzerland, 2001.
14. Tworzewski P., Bacharz K., Michałowska-Maziejuk D. Anchorage Systems in FRP-Strengthened Reinforced Concrete. JCEEA, 2018, 65, 101–110. http://dx.doi.org/10.7862/rb.2018.47 [14]
15. Alobaidi H.E., Al-Zuhairi A.H., Structural strengthening of insufficiently designed reinforced concrete T-beams using CFRP composites. Civil Engineering Journal. 2023, 5, 8, 1880–1896, https://doi.org/10.28991/CEJ-2023-09-08-05
16. Balamuralikrishnan R., Al-Mawaali A.S.H., Al-Yaarubi M.Y.Y., Al-Mukhaini B.B., Kaleem A., Seismic upgradation of RC beams strengthened with externally bonded spent catalyst based ferrocement laminates. HighTech and Innovation Journal. 2023, 4, 1, 189–209. https://doi.org/10.28991/HIJ-2023-04-01-013
17. Mostofinejad D., Mahmoudabadi E., Grooving as alternative method of surface preparation to postpone debonding of FRP Laminates in concrete beams. Journal of Composites for Construction. 2010, 14, 6, 804–811, https://doi.org/10.1061/(ASCE)CC.1943-5614.0000117
18. Abdallaha M., Al Mahmouda F., Boissièrea R., Abdelouahab K., Mercier J. Experimental study on strengthening of RC beams with Side Near Surface Mounted technique-CFRP bars, Composite Structures. 2020, 234, https://doi.org/10.1016/j.compstruct.2019.111716
19. Kotynia R. Przyczepnościowe metody wzmacniania konstrukcji żelbetowych przy użyciu naprężonych kompozytów polimerowych, Przegląd Budowlany, 2015, 7–8, 49–56.
20. De Lorenzis L, Teng JG. Near-surface mounted FRP reinforcement: an emerging technique for strengthening structures. Compos Part B: Engineering, 2007, 38, 2, 119–43. https://doi.org/10.1016/j.compositesb.2006.08.003
21. Ke1 Y., Zhang S. S., Aff. M., Smith S.T., F., Yu T. Novel Embedded FRP Anchor for RC beams strengthened in flexure with NSM FRP bars: Concept and behavior. Journal of Composites for Construction. 2023, 27, 1, https://doi.org/10.1061/(ASCE)CC.1943-5614.0001279
22. Michałowska-Maziejuk D., Goszczyńska B. Effectiveness of strengthening RC beams using composite materials – an accelerated strengthening method; Materials. 2023, 16, 13, https://doi.org/10.3390/

ma16134847

23. Michałowska-Maziejuk D., Goszczyńska B., Szacowanie nośności belek żelbetowych wzmocnionych kompozytami CFRP, Inżynieria i Budownictwo. 2023, 79, 11–12, 636–643, http://dx.doi.org/10.5604/01.3001.0054.1374
24. Hassan T., Rizkalla S. Investigation of bond in concrete structures strengthened with near surface mounted carbon fiber reinforced polymer strips. Journal of Composites for Construction. 2003, 7, 3, 248–257. https://doi.org/10.1061/(ASCE)1090-0268(2003)7:3(248)
25. Peng H., Zhang J., Cai C.S., Liu Y., An experimental study on reinforced concrete beams strengthened with prestressed near surface mounted CFRP strips. Engineering Structures. 2014, 79, 15, 222–233. https://doi.org/10.1016/j.engstruct.2014.08.007
26. Sharaky I.A., Torres L., Comas J., Barris C. Flexural response of reinforced concrete (RC) beams strengthened with near surface mounted (NSM) fibre reinforced polymer (FRP) bars. Composite Structures. 2014, 109, 1, 8–22 https://doi.org/10.1016/j.compstruct.2013.10.051
27. Barros J.A.O., Fortes A.S., Flexural strengthening of concrete beams with CFRP laminates bonded into slits. Cement and Concrete Composites. 2015, 27, 4 471–480. https://doi.org/10.1016/j.cemconcomp.2004.07.004
28. Teng, J.G., De Lorenzis L., Wang B., Li R., Wong T.N., Lam L. Debonding failures of RC beams strengthened with near surface mounted CFRP strips. Journal of Composites for Construction. 2006, 10, 2, pp. 92–105, https://doi.org/10.1061/(ASCE)1090-0268(2006)10:2(92)
29. Seracino R., Jones N.M., Ali M.S., Page M.W., Oehlers D.J. Bond strength of near-surface mounted FRP strip-to-concrete joints. Journal of Composites for Construction. 2007, 11, 4, 401–409,https://doi.org/10.1061/(ASCE)1090-0268(2007)11:4(401)
30. Dias S.J.E., Barros J.A.O., Janwaen W. Behavior of RC beams flexurally strengthened with NSM CFRP laminates. Composite Structures. 2018, 201, 3, 363–376. https://doi.org/10.1016/j.compstruct.2018.05.126
31. Fu B., Tang X.T., Li L.J., Liu F., Lin G., Inclined FRP U-jackets for enhancing structural performance of FRP-plated RC beams suffering from IC debonding, Composite Structures. 2018, 200, 15, 36–46, https://doi.org/10.1016/j.compstruct.2018.05.074
32. Hosen M., Jumaat M.Z., Islam S. Inclusion of CFRP-epoxy composite for end anchorage in NSM-epoxy strengthened beams. Advances in Materials Science and Engineering. 2015, 2015, 1, https://doi.org/10.1155/2015/812797
33. Zhang, S.S., Ke Y., Smith S.T., Zhu H.P., Wang Z.L. Effect of FRP U-jackets on the behaviour of RC beams strengthened in flexure with NSM CFRP strips. Composite Structures. 2021, 256 https://doi.org/10.1016/j.compstruct.2020.113095
34. Khalifa A, Alkhrdaji T, Nanni A, Lansburg A. Anchorage of surface mounted FRP reinforcement. Concrete International, 1999, ACI, 49–54.
35. Kim Y.J., Green M.F., Wight G.R., Prestressed fiber-reinforced polymer (FRP) composites for concrete structures in flexure: fundamentals to applications, Editor(s): Yail J. Kim, Advanced Composites in Bridge Construction and Repair, Woodhead Publishing, 2014, 30-60, https://doi.org/10.1533/9780857097019.1.30
36. Smith S.T., Shenghua Hu, Seo Jin Kim, Seracino R. FRP-strengthened RC slabs anchored with FRP anchors. Engineering Structures, 2011. 33, 4, 1075–1087 https://doi.org/10.1016/j.engstruct.2010.11.018
37. Haddad, R.H., Harb, A.N., Varying profiles of CFRP ropes for strengthening concrete beams. International Journal of Civil Engineering. 2021, 20, 405–419. https://doi.org/10.1007/s40999-021-00664-2
38. Alhilli H.H., Al-Farttoosi M.H., Shear Performance of Reinforced Concrete T Beams Strengthened by Carbon Fiber-Reinforced Polymer Bars. Civil Engineering Journal. 2023, 9, 10, 2411–2429, https://doi.org/10.28991/CEJ-2023-09-10-04
39. Adamczak-Bugno A., Lipiec S., Adamczak J., Vičan J., Bahleda F., Identification of destruction processes and assessment of deformations in compressed concrete modified with polypropylene fibers exposed to fire temperatures using acoustic emission signal analysis, numerical analysis, and digital image correlation. Materials. 2023, 16, 6786. https://doi.org/10.3390/ma16206786
40. Blikharskyy Y., Kopiika N., Khmil R., Selejdak J., Blikharskyy Z. Review of Development and Application of Digital Image Correlation Method for Study of Stress–Strain State of RC Structures. Applied Sciences. 2022, 12, 19, https://doi.org/10.3390/app121910157
41. Bakalarz M.M., Tworzewski P.T., Application of digital image correlation to evaluate strain, stiffness and ductility of full-scale LVL beams strengthened by CFRP. Materials. 2023, 16, 3, 1309, https://doi.org/10.3390/ma16031309
42. Szczecina M., Tworzewski P., Bacharz K., Experimental verification of a numerical model of RC beam with CFRP rope strengthening, Computer Assisted Methods in Engineering and Science, 2019, 26, 3–4, 137–151, http://dx.doi.org/10.24423/cames.269
43. American Concrete Institute ACI. Guide for the design and construction of externally bonded FRP systems for strengthening concrete structures. ACI 440.2R-17, ACI Committee 440, 2017.